Neutrino phenomenology, W-mass anomaly, and muon $(g-2)$ in a minimal type-III seesaw model using a T' modular symmetry

Priya Mishra,[*] Mitesh Kumar Behera,[†] and Rukmani Mohanta[‡]
School of Physics, University of Hyderabad, Hyderabad 500046, India

(Received 6 February 2023; accepted 18 May 2023; published 2 June 2023)

In this study, we introduce a model to illustrate neutrino phenomenology by incorporating two right-handed fermion triplet superfields, i.e., Σ_{R_j}, in the presence of the modular symmetry $\Gamma_3' \simeq A_4'$, a double cover of the A_4 modular symmetry. The motivation in utilizing double cover is that, so far, only even modular forms have been considered for constructing modular invariant models, but, in this case, it is possible to extend the modular invariance approach to general integral weight modular forms, i.e., the odd weight modular forms. Hence, this type of amalgamation between T' modular symmetry and minimally extending the seesaw can correctly explain the neutrino phenomenology. Additionally, we accommodate the most recent measurement of the W-boson mass, published by the CDF-II Collaboration, and shed some light on the recent results of muon $(g-2)$. Finally, we discuss lepton flavor violation in order to establish a constraint on the mass of right-handed fermion.

DOI: 10.1103/PhysRevD.107.115004

I. INTRODUCTION

After the discovery of the Higgs boson, the Standard Model (SM) has gained widespread accomplishment. Numerous experiments have carefully scrutinized the SM predictions, proving it to be a successful theory of electroweak interactions [1]. Although the SM is exceptionally victorious in explaining the interactions up to the electroweak scale, it fails to elucidate mixing patterns in quark and lepton flavor sectors and mass hierarchies amid leptons and quarks, including the nonzero neutrino masses. Hence, using symmetry consideration seems to be the most effective strategy. In support of the above, the non-Abelian discrete flavor symmetry groups have helped us to understand the lepton mixing pattern, whose literature is quite extensive. Discrete flavor symmetries [2–8] combined with generalized CP symmetry [9–12] can lead to fairly predicative models. Notably, the flavor symmetry group, which attempts the explanation of observed quark and lepton flavor mixing patterns, can also accommodate CP symmetry concurrently. For the illustration of nonzero neutrino mass within the roof of SM, a higher-dimensional operator (i.e., dimension five) was pioneered by Weinberg [13]. Because of certain drawbacks associated with higher-dimensional operators, the alternate approach of introducing right-handed (RH) neutrinos became popular, leading to the seesaw mechanism. The exchange of heavy RH particles scales down the mass of neutrinos in a natural way. In support of the above, type-I [14–16], type-II [17–22], and type-III [23–28] seesaw models are based on the exchange of heavy right-handed $\mathrm{SU}(2)_L$ singlet fermions, triplet scalars, and fermionic triplets, respectively. While constructing the models theoretically using discrete flavor symmetries, several flavon fields are required to keep the model invariant under the symmetry groups. These flavon fields also break the flavor symmetry group into different subgroups via their vacuum expectation value (VEV) acquisition, as seen in the neutrino and charged lepton sectors. This often complicates the model, as the leading-order corrections are often subjected to the corrections from higher-dimensional operators as a consequence of utilizing multiple flavon insertions.

The above shortcomings can be pulled off by a recent, yet well-established modular invariance approach [29–32]. As an advantage, flavon fields are not needed anymore or minimized, and the symmetry breaking is performed by the VEV of complex modulus field τ. Consequently, the model can be constructed elegantly by using lesser flavon insertions. In the superpotential, higher-dimensional operators are governed exclusively by modular invariance. It is possible to produce highly predictive models for neutrino masses and mixing angles with modular flavor symmetry. The role of modular forms is played by dimensionless Yukawa couplings, which are functions of modulus τ.

[*]mishpriya99@gmail.com
[†]miteshbehera1304@gmail.com
[‡]rmsp@uohyd.ac.in

Their transformation is governed by the Dedekind eta function instead of being constant in the case of the conventional discrete flavor symmetry approach. Moreover, quark and lepton fields have certain modular weights, which define the nontrivial transformation of these fields under modular forms. As a result, there is a myriad of literature available utilizing finite modular groups, i.e., $\Gamma_2 \simeq S_3$ [33–35], $\Gamma_3(\Gamma_3') \simeq A_4(A_4')$ [36–59], $\Gamma_4 \simeq S_4$ [60–65], $\Gamma_5 \simeq A_5$ [66], and $\Gamma_5' \simeq A_5'$ [67–70]. While setting up the modular invariance approach, the modular weights considered in the assumption are mostly even. However, literature pertaining to the idea of double covering of A_4 symmetry, known as T' symmetry [71], allows both even and odd modular weights for constructing the model.

The main highlight of this work is to accommodate the recent W-mass anomaly reported by the CDF Collaboration, i.e., $m_W^{\text{CDF-II}} = 80.4335 \pm 0.0094$ GeV [72], which establishes a deviation of 7σ from the SM prediction, i.e., $m_W^{\text{SM}} = 80.357 \pm 0.006$ GeV [73]. For the central values, the deviation is $\delta m_W = m_W^{\text{CDF}} - m_W^{\text{SM}} = 0.0765$ GeV, which is quite a fascinating result from the viewpoint of new physics. This observation leads to multiple discussions regarding its potential implications and interpretations, for instance, the Zee model utilizing two Higgs doublets [74], the scotogenic-Zee model [75], type-II Dirac seesaw by adding a vectorlike fermion and real scalar triplet [76], utilizing singlet-doublet fermion [77], and additionally with the minimal supersymmetric SM (MSSM) [78], in the $\mathrm{U}(1)_{L_\mu - L_\tau}$ model with vectorlike leptons which when mixed with the muon can solve this anomaly [79], introduction of one isospin doublet vectorlike lepton [80], the singlet-triplet scotogenic dark matter model [81], vectorlike quark models including the electroweak precision data [82], hadronic contributions by performing electroweak fits [83], and singlet scalar extensions of the SM in the context of the W-boson mass [84]. In the type-III seesaw model, the additional inclusion of a light fermion singlet N and a heavy scalar triplet has significant implications, as discussed in [85]; the scalar triplet is also utilized to explain W mass [86–88].

The organization of this paper is as follows. In Sec. II, we accentuate certain striking features of T' modular symmetry, while in Sec. III, we discuss the model framework containing particles contributing toward expressing the superpotential for type-III seesaw and the associated mass matrices. Subsequently, in Sec. IV, we accomplish the numerical analysis where a mutual parameter space is extracted, satisfying all the phenomena discussed in our model. In Sec. V, we illustrate the W-mass anomaly from CDF-II results, and the recent results of muon $(g-2)$ are discussed in Sec. VI. We have also discussed lepton flavor-violating decay mode $\mu \to e\gamma$ in Sec. VII for obtaining the constraint on the lightest heavy fermion mass M_{R_1}. Finally, in Sec. VIII, we summarize our findings.

II. MODULAR SYMMETRY AS DOUBLE COVER

The modular group Γ_N is a dimension-two finite group (i.e., 2×2 matrices) with integer entries and determinant being unity, also known as $SL(2, Z_N)$ or the homogeneous finite modular group. One can establish the double cover group Γ_N' from Γ_N by including another generator R, which is related to $-\mathrm{I} \in SL(2, Z)$ and commutes with all elements of the $SL(2, Z)$ group, such that the generators S, T, and R of Γ_N' obey certain relations as follows:

$$S^2 = R, (ST)^3 = 1, \qquad T^N = 1,$$
$$R^2 = 1 \quad \text{and} \quad RT = TR. \tag{1}$$

A. $\Gamma_3' \simeq A_4'$ modular symmetry

Since $N = 3$, the dimension of the linear space defined by the computationally efficient mathematical deductions relating to $\Gamma(3)$ is $k+1$, with k being the modular weight. As a result, dimension two is produced if we consider the lowest-order modular weight, $k = 1$. Dedekind's eta function as expressed by Eq. (2) is defined in the upper half plane, i.e., $\mathcal{H} = \{\tau \in \mathbb{C} | \mathrm{Im}(\tau) > 0\}$, and is what creates the modular space

$$\eta(\tau) = q^{1/24} \prod_{i=1}^{\infty} (1 - q^n), \qquad q \equiv e^{2\pi i \tau}. \tag{2}$$

Also, the generators T and S transform η as

$$\eta(\tau + 1) = e^{i\pi/12} \eta(\tau), \qquad \eta(-1/\tau) = \sqrt{-i\tau}\, \eta(\tau). \tag{3}$$

We are working in the linear space of $\Gamma(3)$, whose expression depending upon η is given by [89]

$$\mathcal{M}_k(\Gamma(3)) = \bigoplus_{a+b=k, a,b \geq 0} \mathbb{C} \frac{\eta^{3a}(3\tau) \eta^{3b}(\tau/3)}{\eta^k(\tau)}. \tag{4}$$

As the dimension of $\mathcal{M}_k(\Gamma(3))$ is $k+1$, for $k = 1$ we can take the basis vectors to be

$$\hat{e}_1(\tau) = \frac{\eta^3(3\tau)}{\eta(\tau)}, \qquad \hat{e}_2(\tau) = \frac{\eta^3(\tau/3)}{\eta(\tau)}.$$

The basis vectors shown above are linearly independent, and any modular forms of $k = 1$ and $N = 3$ can be expressed as a linear combination of $\hat{e}_1$ and $\hat{e}_2$. Further, due to application of generator T, $\hat{e}_i$ $(i = 1, 2)$ transform as

$$\hat{e}_1(\tau) \overset{T}{\mapsto} e^{i2\pi/3} \hat{e}_1(\tau), \quad \hat{e}_2(\tau) \overset{T}{\mapsto} 3(1 - e^{i2\pi/3}) \hat{e}_1 + \hat{e}_2. \tag{5}$$

TABLE I. Particle content of the model and their charges under $\mathrm{SU}(2)_L \times \mathrm{U}(1)_Y \times T'$ group and their modular weights k_I.

Fields	E^c_{1R}	E^c_{2R}	E^c_{3R}	l_{L_i}	Σ^c_R	$H_{u,d}$
$\mathrm{SU}(2)_L$	1	1	1	2	3	2
$\mathrm{U}(1)_Y$	1	1	1	$-\frac{1}{2}$	0	$\frac{1}{2}, -\frac{1}{2}$
T'	1	$1'$	$1''$	$1, 1'', 1'$	2	1
k_I	-2	-2	-2	2	3	0

Similarly, under generator S,

$$\hat{e}_1(\tau) \overset{S}{\mapsto} 3^{-3/2}(-i\tau)\hat{e}_2(\tau), \quad \hat{e}_2(\tau) \overset{S}{\mapsto} 3^{3/2}(-i\tau)\hat{e}_1(\tau). \tag{6}$$

Therefore, utilizing the above information, one will be able to construct a modular multiplet $Y^{(1)}_{\mathbf{2}}$ that transforms as a doublet $\mathbf{2}$ under $\Gamma'_3 \cong T'$ involving the basis vectors $\hat{e}_1$ and $\hat{e}_2$,

$$Y^{(1)}_{\mathbf{2}}(\tau) = \begin{pmatrix} Y_1(\tau) \\ Y_2(\tau) \end{pmatrix}, \tag{7}$$

with

$$Y_1(\tau) = \sqrt{2}e^{i7\pi/12}\hat{e}_1(\tau), \quad Y_2(\tau) = \hat{e}_1(\tau) - \frac{1}{3}\hat{e}_2(\tau). \tag{8}$$

Further, the higher weight modular Yukawa couplings with $k = 2$, 3, 4, 5 can be constructed from the tensor product of $Y^{(1)}_{\mathbf{2}}$ (see Ref. [71]). Also the complete form of other doublet Yukawa couplings are mentioned in the Appendix. References [90–92] also discuss the double covering of group Γ_N.

III. MODEL FRAMEWORK

To incorporate a minimal type-III seesaw in our model, we have added right-handed hyperchargeless ($Y = 0$) fermionic triplet superfields $\Sigma^c_{R_j}$ ($j = 1$, 2), which transform as a triplet under $\mathrm{SU}(2)_L$ and a doublet under T' modular symmetry with $k_I = 3$. Further, Higgs supermultiplets $H_{u,d}(Y = \pm 1/2)$ are singlets under T' modular symmetry with zero modular weight. The VEVs of Higgs supermultiplets, i.e., (v_u, v_d) are related to the SM Higgs VEV (v_H) by a simple equation $v_H = \frac{1}{2}\sqrt{v_u^2 + v_d^2}$. The ratio of Higgs supermultiplet VEVs is written as $\tan\beta = (v_u/v_d) \simeq 5$ (used in our analysis) [93–95]. The SM right-handed charged leptons E^c_{1R}, E^c_{2R}, and E^c_{3R} transform as $1, 1'$, and $1''$ under T' modular symmetry with $k_I = -2$. While, left-handed lepton doublets $l_{Li}(i = e, \mu, \tau)$ transform as $1, 1''$, and $1'$ under T' symmetry, respectively, with $k_I = 2$ represented in Table I.

The complete superpotential is given by

$$\begin{aligned}\mathcal{W} = {} & \sqrt{2}y_\ell l_{L_i} H_d E^c_{R_i} + \alpha_D\left[Y^{(5)}_{\wp} H_u^T \eta (\Sigma^c_{R_j} l_{L_i})_{\wp'}\right] \\ & + \frac{M_\Sigma \alpha_\Sigma}{2}\mathrm{Tr}\left[\sum_{j=1}^{2} \Sigma^c_{R_j}\lambda_1 \Sigma^c_{R_j}\right] \\ & + \mu H_u H_d + \lambda_1 M_{\tilde{\Sigma}} \mathrm{Tr}[\tilde{\Sigma}_j \tilde{\Sigma}_j] + \lambda_2 [H_u^T \eta \tilde{\Sigma}_1 H_d],\end{aligned} \tag{9}$$

where $\wp = (\mathbf{2}'', \mathbf{2}, \mathbf{2}')$, $\wp' = (\mathbf{2}, \mathbf{2}'', \mathbf{2}')$ with $\alpha_{\Sigma(D)}$ and $\Sigma^c_{R_j}$ are defined as

$$\Sigma^c_{R_j} = \frac{1}{\sqrt{2}}\begin{pmatrix} \Sigma^{0c}_j & \sqrt{2}\Sigma^{+c}_j \\ \sqrt{2}\Sigma^{-c}_j & -\Sigma^{0c}_j \end{pmatrix},$$

$$\alpha_{\Sigma(D)} = \begin{pmatrix} g_{\Sigma_1(D_1)} & 0 \\ 0 & g_{\Sigma_2(D_2)} \end{pmatrix}, \quad \eta = \begin{pmatrix} 0 & 1 \\ -1 & 0 \end{pmatrix}, \tag{10}$$

with $\alpha_{\Sigma(D)}$ being the free parameter matrices, whereas M_Σ is the free mass parameter and $\tilde{\Sigma}_j$ is the scalar superpartner of triplet superfield (Σ_{R_j}). Further, λ_1 and λ_2 are the couplings with modular forms given in the Appendix. Table II contains the modular weights of the Yukawa couplings ($Y^{(5)}_{\wp}$) with ($\wp = (\mathbf{2}, \mathbf{2}', \mathbf{2}'')$), λ_1 and λ_2 along with their transformation under T' symmetry. Moreover, the charged lepton superpotential term as shown by the first part in Eq. (9) yields a mass matrix (i.e., diagonal) exactly of the form as elaborated in Ref. [59]. Hence, we focus on the neutral lepton sector, as discussed below.

A. Dirac mass term

The Dirac mass matrix for the neutral lepton sector can be obtained from the following superpotential term:

$$\mathcal{W}_D = \alpha_D\sqrt{2}\left[Y^{(5)}_{\mathbf{2}'',\mathbf{2},\mathbf{2}'} H_u^T \eta (\Sigma^c_{R_j} l_{L_i})_{\mathbf{2},\mathbf{2}'',\mathbf{2}'}\right]. \tag{11}$$

As H_u gains the VEV, the neutral leptons obtain their masses. To make the Dirac term invariant, fermion triplets transform as a doublet under T' modular symmetry. Hence, the Dirac interaction term of a neutral multiplet of a fermion

TABLE II. Charge assignment to Yukawa couplings under T' and its modular weight k_I.

Couplings	$Y^{(5)}_{2,I} = (y_{12}, y_{22})$	$Y^{(5)}_{2',I} = (y_{12'}, y_{22'})$	$Y^{(5)}_{2'',I} = (y_{12''}, y_{22''})$	$\lambda_1 = Y^{(6)}_{3,I} = (y_{13}, y_{23}, y_{33})$	$\lambda_2 = Y^{(3)}_{2''}$
T'	2	$2'$	$2''$	3	$2''$
k_I	5	5	5	6	3

TABLE III. The NuFIT values of the oscillation parameters along with their $1\sigma/3\sigma$ ranges.

Oscillation parameters	Best fit value $\pm 1\sigma$	3σ range
$\Delta m^2_{21}(10^{-5}\ \mathrm{eV}^2)$	$7.41^{+0.21}_{-0.20}$	6.82–8.03
$\lvert\Delta m^2_{31}\rvert(10^{-3}\ \mathrm{eV}^2)$ (NO)	$2.507^{+0.026}_{-0.027}$	2.427–2.59
$\sin^2\theta_{12}$	$0.303^{+0.012}_{-0.012}$	0.27–0.341
$\sin^2\theta_{23}$ (NO)	$0.451^{+0.019}_{-0.016}$	0.408–0.603
$\sin^2\theta_{13}$ (NO)	$0.02225^{+0.00056}_{-0.00059}$	0.02052–0.02398
$\delta_{CP}/°$ (NO)	232^{+36}_{-26}	144–350

triplet with the SM left-handed neutral leptons can be written as

$$M_D = v_u \begin{bmatrix} y_{22''} & -y_{22} & -y_{22'} \\ -y_{12''} & y_{12} & y_{12'} \end{bmatrix}. \tag{12}$$

B. Majorana mass term

The superpotential for the Majorana mass term for right-handed neutrinos is given as

$$\mathcal{W}_R = \frac{\alpha_\Sigma M_\Sigma}{2}\mathrm{Tr}\left[\sum_{j=1}^{2}\Sigma^c_{R_j}\lambda_1\Sigma^c_{R_j}\right], \tag{13}$$

where M_Σ is the free mass parameter, and application of the A'_4 product rule yields the mass structure given as follows:

$$M_R = \frac{M_\Sigma}{\sqrt{2}}\begin{bmatrix} g_{\Sigma_1} & 0 \\ 0 & g_{\Sigma_2} \end{bmatrix}\begin{bmatrix} \sqrt{2}e^{5\pi i/12}y_{23} & -y_{33} \\ -y_{33} & \sqrt{2}e^{7\pi i/12}y_{13} \end{bmatrix}. \tag{14}$$

Thus, the active neutrino mass matrix in the framework of the type-III seesaw is given as

$$m_\nu = -M_D^T M_R^{-1} M_D. \tag{15}$$

IV. NUMERICAL ANALYSIS

The neutrino oscillation data from NuFIT [96,97] within their 3σ range serves as the reference for the numerical analysis for our model framework, as given in Table III. The neutrino mass formula presented in Eq. (15) leads to the deduction of the associated mass matrix on which numerical diagonalization is performed using the relation $\mathcal{U}^\dagger\mathcal{M}\mathcal{U} = \mathrm{diag}(m^2_{\nu_1}, m^2_{\nu_2}, m^2_{\nu_3})$, where $\mathcal{M} = m_\nu m_\nu^\dagger$, and $\mathcal{U}$ is the unitary matrix, from which the neutrino mixing angles can be derived using the conventional relations,

$$\sin^2\theta_{13} = |\mathcal{U}_{13}|^2, \qquad \sin^2\theta_{12} = \frac{|\mathcal{U}_{12}|^2}{1-|\mathcal{U}_{13}|^2},$$
$$\sin^2\theta_{23} = \frac{|\mathcal{U}_{23}|^2}{1-|\mathcal{U}_{13}|^2}. \tag{16}$$

Another intriguing observable related to the mixing angles and phases of the Pontecorvo-Maki-Nakagawa-Sakata (PMNS) matrix is the Jarlskog invariant, expressed as

$$J_{CP} = \mathrm{Im}[\mathcal{U}_{e1}\mathcal{U}_{\mu 2}\mathcal{U}^*_{e2}\mathcal{U}^*_{\mu 1}] = s_{23}c_{23}s_{12}c_{12}s_{13}c^2_{13}\sin\delta_{CP}. \tag{17}$$

Further, we chose the following model parameter ranges to fit the present neutrino oscillation data:

$$\mathrm{Re}[\tau] \in [-0.5, 0.5], \qquad \mathrm{Im}[\tau] \in [0.75, 2],$$
$$M_\Sigma \in [10^4, 10^5]\ \mathrm{TeV},$$
$$\alpha_D \in [10^{-5}, 10], \qquad \alpha_\Sigma \in [10^{-2}, 10^{-1}]. \tag{18}$$

We consider the free mass parameter (M_Σ), real and imaginary parts of τ, and free parameters α_D and α_Σ to vary randomly in their corresponding ranges[1] given in Eq. (18). The ranges for τ's real and imaginary parts are varied within $[-0.5, 0.5]$ and [0.75, 2], respectively. We noticed that the model satisfies the normal ordering (NO) scheme. We arbitrarily examine the parameter input values based on these ranges, hence, we are able to simultaneously satisfy the constraints on the sum of neutrino masses obtained from Planck data [98,99], in the context of the present model framework.

As a result, the left panel of Fig. 1 projects the interdependence between $\sin^2\theta_{13}$ (i.e., varying within [0.02052–0.02398]) with respect to the sum of neutrino masses ($\sum m_{\nu_i}$), where the value of $\sum m_{\nu_i}$ is found to be above its lower bound, i.e., 0.058 eV [98,100], obtained for NO and assuming the lightest neutrino mass to be quite small. The right panel of Fig. 1 shows the interdependence of $\sum m_{\nu_i}$ with $\sin^2\theta_{12}(\sin^2\theta_{23})$, where it is seen that $\sin^2\theta_{12}$ satisfies a very narrow region of [0.311–0.341] and $\sin^2\theta_{23}$ is within the range [0.408–0.603]. Further, Fig. 2(a) shows the interdependence of $\sin^2\theta_{13}$ with CP phase δ_{CP}, which varies within $[142.1° - 283°]$, whereas Fig. 2(b) expresses the correlation of M_{R_1} and M_{R_2}, i.e., heavy fermion masses, and is found to be hierarchical, where M_{R_1} lies between [0.5–13.4] TeV, and the lower limit obtained for M_{R_2} is 128.8 TeV going up to 5530 TeV. Finally, in Fig. 2(c), we depict the correlation of reactor

[1]It is to be noted here that, as seven free parameters [i.e., 2D matrices—(α_Σ, α_D), Re(τ), Im(τ), M_Σ] are being varied randomly to illustrate the observed oscillation data by imposing certain constraint conditions, the obtained correlations between different measured parameters are less prominent.

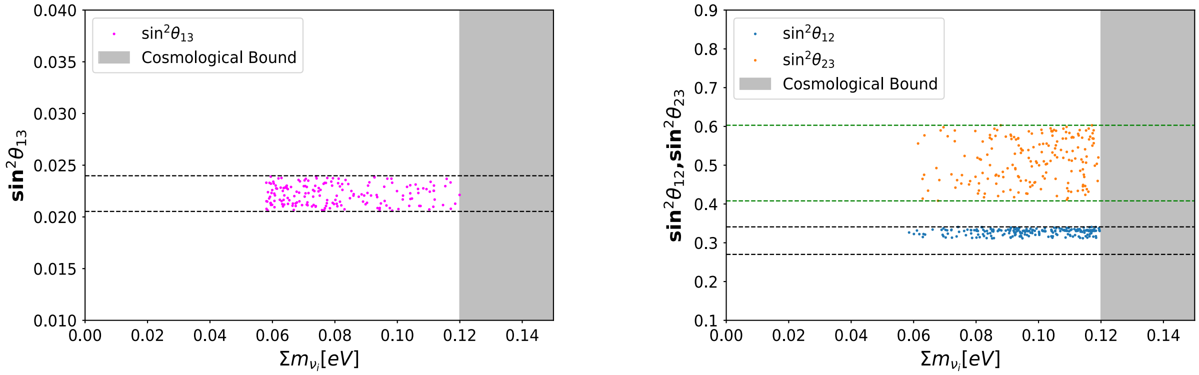

FIG. 1. Left (right): the plane of the mixing angles, i.e., $\sin^2\theta_{13}$ ($\sin^2\theta_{12}$ and $\sin^2\theta_{23}$) with the sum of neutrino masses for the aforementioned ranges of model parameters. Horizontal grid lines represent the 3σ range of mixing angles, with the gray band being the excluded region from the cosmological bound (i.e., $\sum m_i \geq 0.12$ eV).

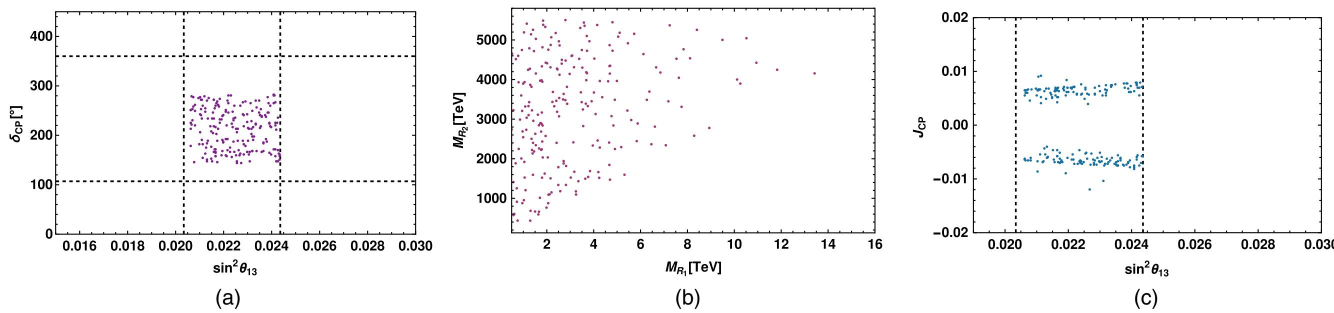

FIG. 2. Panel (a) (Panel (c)): expresses the correlation between δ_{CP} (J_{CP}) with respect to mixing angle $\sin^2\theta_{13}$. Panel (b): depicts the correlation between heavy neutrino mass M_{R_1} and M_{R_2} in TeV scale.

mixing angle with the Jarlskog invariant and see that $|J_{CP}| \leq 0.01$ with $\sin^2\theta_{13}$ within its 3σ range. Proceeding further, in Fig. 3, we depict the correlation of Re(τ) and Im (τ) with mixing angles [i.e., Fig. 3(a), $\sin^2\theta_{13}$; Fig. 3(b), $\sin^2\theta_{12}$; and Fig. 3(c), $\sin^2\theta_{23}$] due to the fact that there is an implicit relation of oscillation parameters with modulus τ.

V. W-MASS ANOMALY

The W-mass anomaly, associated with the recent measurement of its value by the CDF-II Collaboration [72], indicates the role of physics beyond the Standard Model (BSM). Considering this discrepancy is just a consequence of the BSM, we assume the mass of the W boson gets an immediate effect in the presence of the scalar superpartner of the triplet superfield, i.e., ($\tilde{\Sigma}_i$), whereas the mass of the Z boson remains unchanged [81,101]. Because of the hierarchical nature of fermion triplets, as shown in the upper right panel of Fig. 2, it is assumed that the mass of scalar triplets ($\tilde{\Sigma}_j$) is also hierarchical. So, the VEV of the smallest scalar field will contribute positively to explain updated W mass by CDF-II. The soft breaking terms in the presence of $\tilde{\Sigma}_1$, in addition to the MSSM soft breaking term, are [102,103] given as follows:

$$-\mathcal{L} = m^2_{H_u}|H_u|^2 + m^2_{H_d}|H_d|^2 + bH_uH_d + 2a^2_{\tilde{\Sigma}}\lambda_1 \mathrm{Tr}(\tilde{\Sigma}_1\tilde{\Sigma}_1) + 2\lambda_2 B_\lambda(H_u^T\eta\tilde{\Sigma}_1 H_d), \tag{19}$$

where $m^2_{H_u}$, $m^2_{H_d}$, b, $a^2_{\tilde{\Sigma}}$, and B_λ are soft breaking parameters, and $\lambda_1(\lambda_2)$ have modular form with $k_I = 3(6)$ and transform as a doublet under T' symmetry, as defined in Eqs. (A6) and (A7) in the Appendix. The scalar potential at the tree level can be written as

$$V = (m^2_{H_u} + \mu^2)|H^0_u|^2 + (m^2_{H_d} + \mu^2)|H^0_d|^2 + \lambda_1(a^2_{\tilde{\Sigma}} + \lambda_1 M^2_{\tilde{\Sigma}})|\tilde{\Sigma}^0_1|^2 - bH^0_uH^0_d + (B_\lambda - 2\lambda_1 M_{\tilde{\Sigma}})\lambda_2(H^0_u\tilde{\Sigma}^0_1H^0_d)$$
$$+ \lambda_2^2|\tilde{\Sigma}^0_1|^2(|H^0_u|^2 + |H^0_d|^2) + 2\mu\lambda_2\tilde{\Sigma}^0_1(|H^0_u|^2 + |H^0_d|^2) + \lambda_2^2|H^0_d|^2|H^0_u|^2 + \frac{1}{8}(g_1^2 + g_2^2)(|H^0_u|^2 - |H^0_d|^2)^2. \tag{20}$$

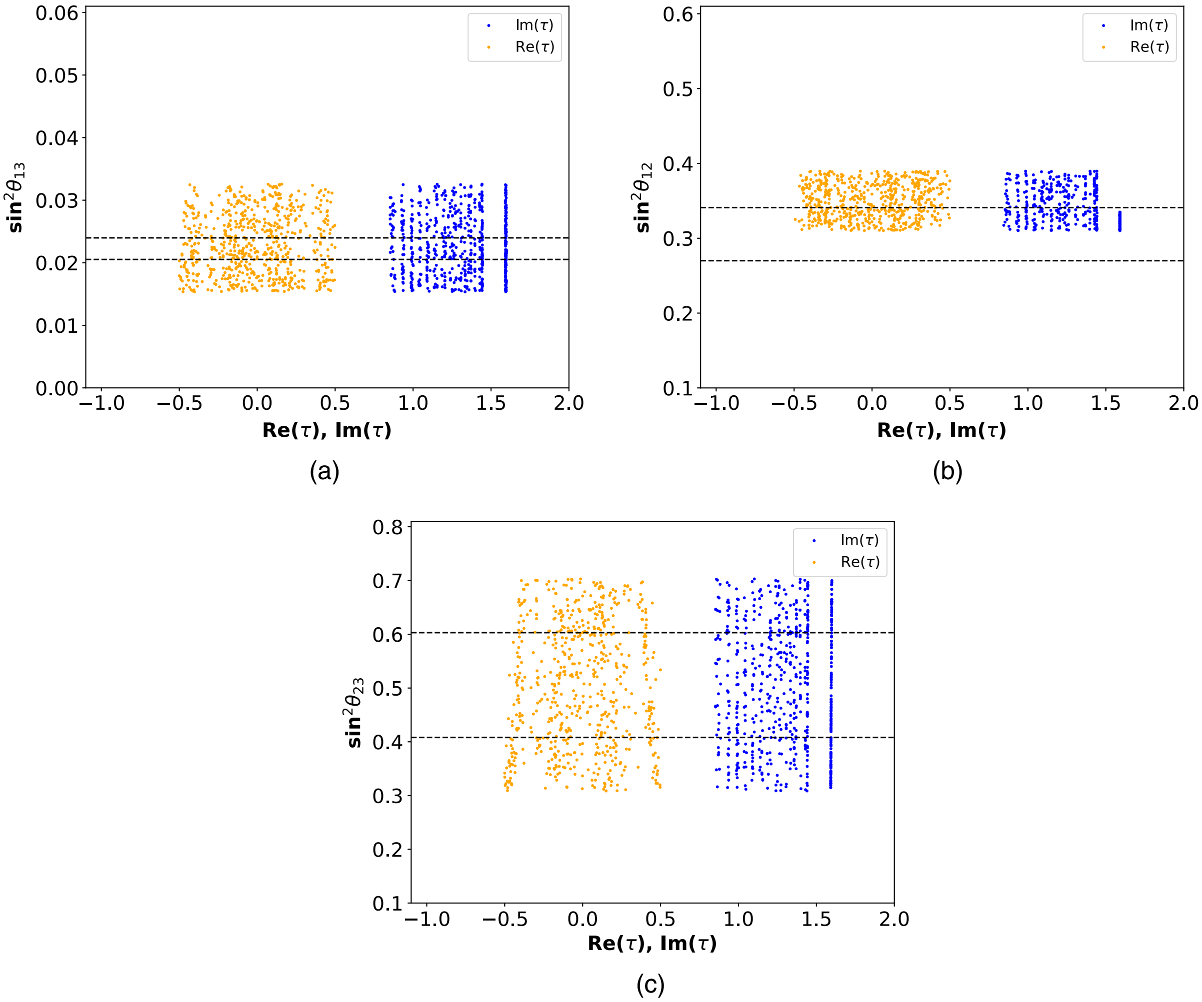

FIG. 3. (a)–(c) Correspond to correlation of Re(τ) and Im(τ) with mixing angles $\sin^2\theta_{13}$, $\sin^2\theta_{12}$, and $\sin^2\theta_{23}$, respectively.

The terms containing μ^2 as its coefficient come from an F-term, whereas g_1 and g_2 are gauge couplings, resulting from the D-term contribution to the scalar potential [102]. After minimizing the scalar potential, we get the following conditions, which are utilized in the calculations of the mass of real part of Higgs, as elaborated in Sec. V A:

$$m_{H_u}^2 = \frac{b\cot\beta}{2} - \mu^2 - \frac{\lambda_2}{2\sqrt{2}}(B_\lambda - 2\lambda_1 M_{\tilde{\Sigma}})v_{\tilde{\Sigma}_1^0}\cot\beta - \frac{\lambda_2^2}{2}(v_{\tilde{\Sigma}_1^0}^2 + v_d^2) - \sqrt{2}\mu\lambda_2 v_{\tilde{\Sigma}_1^0} - \frac{1}{8}(g_1^2+g_2^2)(v_u^2 - v_d^2),$$
$$m_{H_d}^2 = \frac{b\tan\beta}{2} - \mu^2 - \frac{\lambda_2}{2\sqrt{2}}(B_\lambda - 2\lambda_1 M_{\tilde{\Sigma}})v_{\tilde{\Sigma}_1^0}\tan\beta - \frac{\lambda_2^2}{2}(v_{\tilde{\Sigma}_1^0}^2 + v_u^2) - \sqrt{2}\mu\lambda_2 v_{\tilde{\Sigma}_1^0} + \frac{1}{8}(g_1^2+g_2^2)(v_u^2 - v_d^2). \tag{21}$$

The VEV of $\tilde{\Sigma}_1^0$ can be written as

$$v_{\tilde{\Sigma}_1^0} = \frac{\lambda_2}{\lambda_1\sqrt{2}}\left(\frac{\left(\lambda_1 M_{\tilde{\Sigma}} - \frac{B_\lambda}{2}\right)v_u v_d - \mu v_H^2}{\lambda_1 M_{\tilde{\Sigma}}^2 + a_{\tilde{\Sigma}}^2 + \frac{\lambda_2^2}{2}v_H^2}\right), \tag{22}$$

which ultimately contributes only to the mass of the W boson, while the Z mass remains unchanged, as depicted below,

$$M_W^2 = \frac{1}{4}g_2^2(v_H^2 + v_{\tilde{\Sigma}_1^0}^2), \qquad M_Z^2 = \frac{v_H^2(g_1^2+g_2^2)}{4}. \tag{23}$$

We scan the assumed parameters in the following ranges [103]:

$$\mu = [100, 200]\ \text{GeV}, \qquad B_\lambda = [1, 2\times 10^6]\ \text{TeV},$$
$$a_\Sigma = [1, 10^3]\ \text{TeV},$$
$$M_{\tilde{\Sigma}} = [10, 100]\ \text{TeV}, \qquad b = [10^2, 10^4]\ \text{TeV}^2. \tag{24}$$

In order to account for the new CDF-II result for the W-boson mass, the VEV of $\tilde{\Sigma}_1^0$ must lie within a specific range. This range is identified as 3.5–4.4 GeV and is shown in the upper left panel of Fig. 4, from the variation of M_W with the $v_{\tilde{\Sigma}_1^0}$. Also, under the roof of the SM, the ρ parameter value is given as

$$\rho_{\text{SM}} = 1.00038 \pm 0.00020, \tag{25}$$

and the updated values of the ρ parameter due to W mass from the CDF-II result are

$$\rho_{\text{CDF}} = \frac{M_W^2}{M_Z^2 \cos^2\theta_w} = 1.00179. \tag{26}$$

We can define the ρ parameter in terms of VEVs of $\tilde{\Sigma}^0$, H_u, and H_d,

$$\rho = 1 + 8\frac{v_{\tilde{\Sigma}_1^0}^2}{v_H^2}. \tag{27}$$

It is worth noting that Eqs. (26) and (27) provide the value of $v_{\tilde{\Sigma}_1^0} \simeq 3.5$ GeV, which falls within the specified range illustrated in the upper left panel of Fig. 4. We show the correlation between B_λ and a_Σ, imposing the constraint of 3σ range of W mass, for two specific values of $\mu = 100$ and 200 GeV, and the result is shown in upper right panel of Fig. 4, which indicates that there is not much difference for both values of μ. Therefore, we adopt a benchmark value of $\mu = 150$ GeV to explore the dependence of other parameters on the mass of the W boson. To achieve this, we employed three benchmark values of a_Σ, as 200, 500, and 800 TeV, to get a good correlation between M_W and B_λ, as shown in the lower left panel of Fig. 4. From this figure, it should be noted that, as the value of a_Σ increases, the allowed range of B_λ also increases, which can also be inferred from the top right panel of Fig. 4. Similar behavior can also be noticed, if we consider three representative values for B_λ: 2×10^5, 6×10^5, and 8×10^5 TeV, to obtain a correlation between M_W and a_Σ, as shown in the lower right panel of Fig. 4.

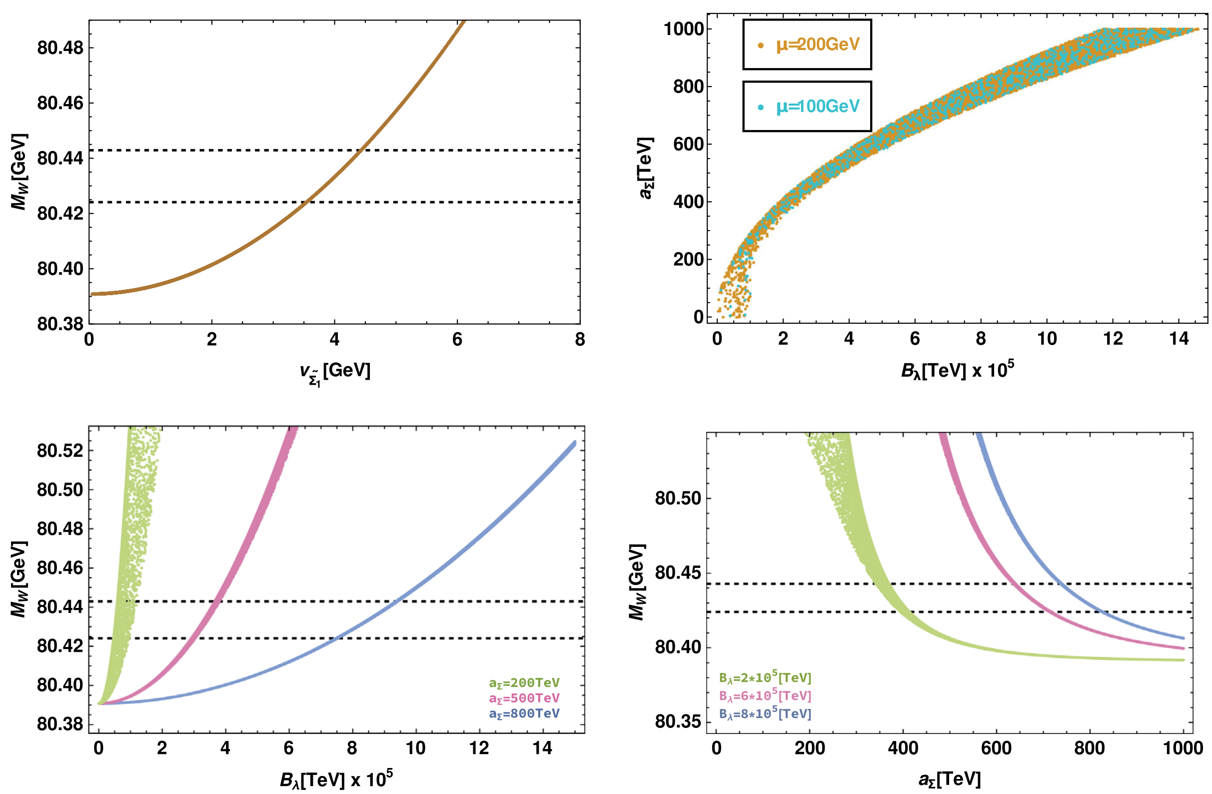

FIG. 4. The plot in the upper left displays the permissible range of VEV for the scalar triplet $\tilde{\Sigma}_1$, which can elucidate the anomaly in the W-boson mass. The upper right plot demonstrates the interdependence between B_λ and a_Σ when restricted to the 3σ constraint of the W-boson mass. In the lower left (right) plot, the behavior of B_λ (a_Σ) with respect to M_W is presented for three distinct values, each represented by a different color. In all of these plots, the value of μ has been held constant at 150 GeV.

A. Mass of *CP* even Higgs

The neutral components of scalars can be written in terms of the real and imaginary parts as follows:

$$H_u^0 = \frac{(H_{uR} + v_u) + iH_{uI}}{\sqrt{2}}, \tag{28}$$

$$H_d^0 = \frac{(H_{dR} + v_d) + iH_{dI}}{\sqrt{2}}, \tag{29}$$

$$\tilde{\Sigma}_1^0 = \frac{(t_R + v_{\tilde{\Sigma}_1^0}) + it_I}{\sqrt{2}}, \tag{30}$$

where H_{uR}, H_{dR}, and t_R are real and H_{uI}, H_{dI}, and t_I are imaginary parts of fields H_u^0, H_d^0, and $\tilde{\Sigma}_1^0$, respectively. After electroweak symmetry breaking, the symmetric mass matrix for the *CP* even Higgs can be written in the basis of (H_{uR}, H_{dR}, t_R),

$$M^2_{CP\text{ even}} = \begin{pmatrix} m_{11}^2 & m_{12}^2 & m_{13}^2 \\ m_{21}^2 & m_{22}^2 & m_{23}^2 \\ m_{31}^2 & m_{32}^2 & m_{33}^2 \end{pmatrix}, \tag{31}$$

with the matrix elements m_{ij}^2 as

$$\begin{aligned}
m_{11}^2 &= m_{H_u}^2 + \mu^2 + \frac{\lambda_2^2}{2}(v_{\tilde{\Sigma}_1^0}^2 + v_d^2) + \frac{1}{8}(g_1^2 + g_2^2)(3v_u^2 - v_d^2) + \sqrt{2}\lambda_2\mu v_{\tilde{\Sigma}_1^0}, \\
m_{22}^2 &= m_{H_d}^2 + \mu^2 + \frac{\lambda_2^2}{2}(v_{\tilde{\Sigma}_1^0}^2 + v_u^2) + \frac{1}{8}(g_1^2 + g_2^2)(3v_d^2 - v_u^2) + \sqrt{2}\lambda_2\mu v_{\tilde{\Sigma}_1^0}, \\
m_{33}^2 &= \lambda_1(\lambda_1 M_{\tilde{\Sigma}}^2 + a_{\tilde{\Sigma}}^2) + \frac{1}{2}\lambda_2^2 v_H^2, \\
m_{12}^2 &= \lambda_2^2 v_u v_d - \frac{b}{2} - \frac{1}{4}(g_1^2 + g_2^2)v_u v_d + \frac{\lambda_2}{2\sqrt{2}} v_{\tilde{\Sigma}_1^0}(B_\lambda - 2\lambda_1 M_{\tilde{\Sigma}}), \\
m_{13}^2 &= \frac{\lambda_2}{2\sqrt{2}} v_d(B_\lambda - 2\lambda_1 M_{\tilde{\Sigma}}) + \lambda_2^2 v_{\tilde{\Sigma}_1^0} v_u + \sqrt{2}\mu\lambda_2 v_u, \\
m_{23}^2 &= \frac{\lambda_2}{2\sqrt{2}} v_u(B_\lambda - 2\lambda_1 M_{\tilde{\Sigma}}) + \lambda_2^2 v_{\tilde{\Sigma}_1^0} v_d + \sqrt{2}\mu\lambda_2 v_d.
\end{aligned} \tag{32}$$

Since $M^2_{CP\text{ even}}$ is a symmetric matrix, we have $m_{ij}^2 = m_{ji}^2$ and the expressions for m_{11}^2 and m_{22}^2 can be simplified further by using Eq. (21). Diagonalization of the matrix $M^2_{CP\text{ even}}$ provides mass for the real part of Higgs in basis (h, H, A). Figure 5 illustrates the constraints obtained on the masses of these three scalars using the current observation of W mass. From the figure, we obtain limits on their masses as $m_h \in [124.74, 125.76]$ GeV, corresponding to the SM Higgs, while $m_H \in [6.6, 65.7]$ and $m_A \in [18.7, 140.8]$ TeV.

VI. MUON $(g-2)$

The triumph of the quantum field theory brings muon anomalous magnetic moment $(g-2)$ into the limelight. The convincing difference between measurements and predictions of the SM could also portend new physics since it has historically drawn much attention. The SM contribution quantified so far is given as [104–123]

$$(a_\mu)^{\text{SM}} = 116591810(43) \times 10^{-11}. \tag{33}$$

As part of its April 2021 announcement, Fermilab reported its first measurement on the muon anomalous magnetic dipole moment [124] given as

$$(a_\mu)^{\text{FNAL}} = 116592040(54) \times 10^{-11}, \tag{34}$$

which contradicts SM results by 3.3σ and simultaneously agrees with the Brookhaven National Laboratory E821 results [125,126],

$$(a_\mu)^{\text{BNL}} = 11659208.0(6.3) \times 10^{-10}. \tag{35}$$

The size of the difference between the average of both experiments and SM prediction is

$$\Delta a_\mu = (a_\mu)^{\text{exp}} - (a_\mu)^{\text{SM}} = (251 \pm 59) \times 10^{-11}, \tag{36}$$

at 4.2σ level. This deviation is significantly large enough, pointing toward the possible role of new physics. In this context, we show the new fermionic triplet $\Sigma_{R_1}^c$ could be a potential candidate for explaining $(g-2)_\mu$ discrepancy. The relevant contribution is shown in Fig. 6, obtained from the corresponding superpotential term, i.e., the second term in Eq. (9).

Thus, we obtain the additional contribution to muon $(g-2)$ as [127]

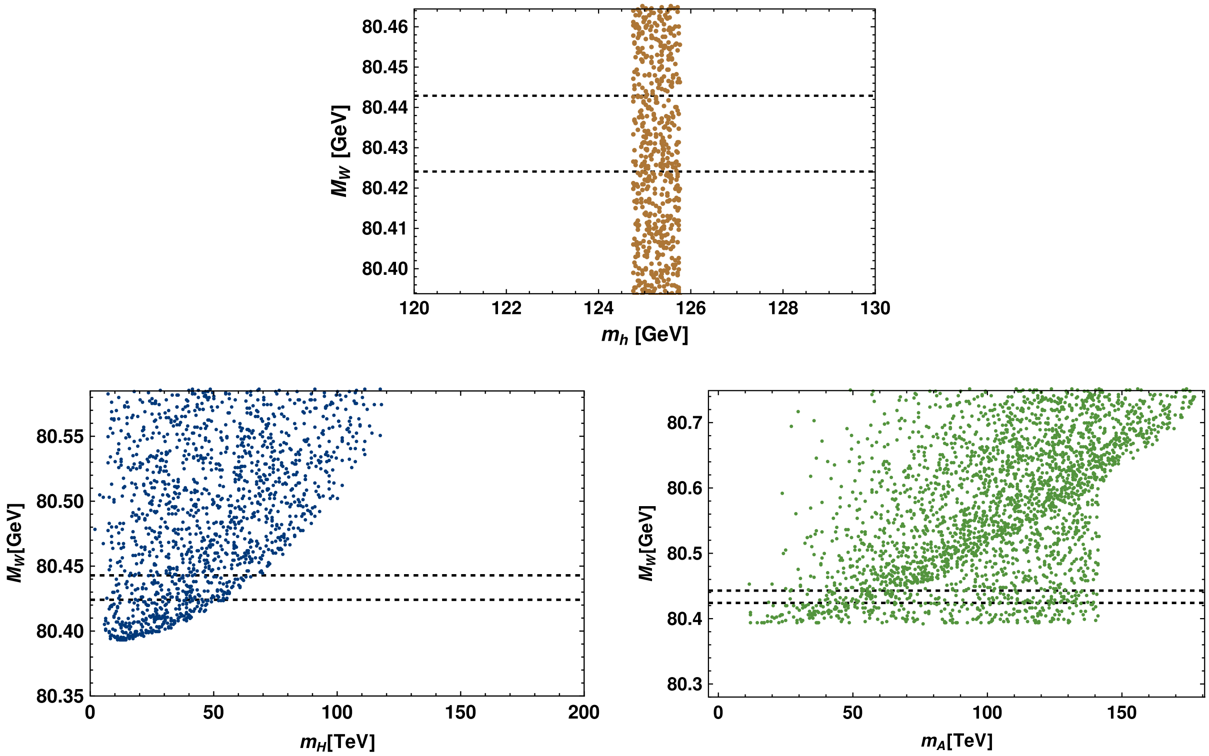

FIG. 5. Top: a limit on the mass of the smallest scalar particle that has been obtained by imposing the mass of the W boson. Lower left (right): shows the limit bounded on BSM scalars m_H (m_A) through W mass.

$$\Delta a_\mu = \frac{m_\mu^2}{32\pi^2 m_h^2}\{(2|g_{D_1}y_{22}|^2)F_h(x_1) + z_1 \mathrm{Re}[(g_{D_1}y_{22})^2]G_h(x_1)\}, \tag{37}$$

where $x_1 = \frac{M_{R_1}^2}{m_h^2}$, $z_1 = \frac{M_{R_1}}{m_\mu}$, and g_{D_1} is free parameter defined in Eq. (10). The loop functions are expressed as

$$F_h(x_1) = \frac{x_1^3 - 6x_1^2 + 3x_1 + 2 + 6x_1 \ln(x_1)}{6(1-x_1)^4}, \tag{38}$$

$$G_h(x_1) = \frac{-x_1^2 + 4x_1 - 3 - 2\ln(x_1)}{(1-x_1)^3}. \tag{39}$$

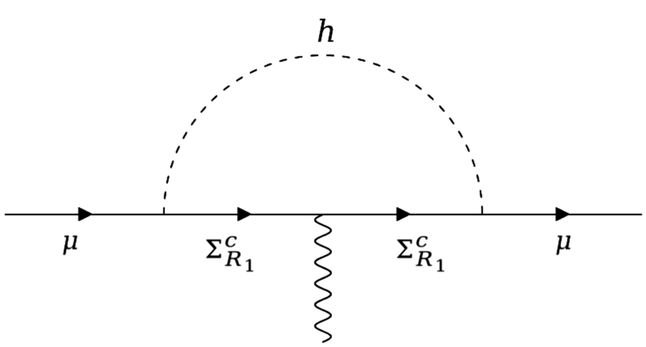

FIG. 6. Feynman diagram involving additional fermion triplet $\Sigma_{R_1}^c$ that generates a muon anomalous magnetic moment.

As the right-handed triplets have hierarchical mass, only the lightest heavy fermion $\Sigma_{R_1}^c$ contributes toward muon anomalous magnetic moment. The correlational behavior of the mass of $\Sigma_{R_1}^c$ with respect to Δa_μ for $m_h = 125.25$ GeV is shown in Fig. 7.

Next, we would like to see the common allowed ranges on the values of real and imaginary parts of the modulus τ compatible with the neutrino oscillation phenomenology, W mass, and muon $(g-2)$. In Fig. 8, we present a plot illustrating the corresponding allowed parameter space compatible with W mass (represented by blue points),

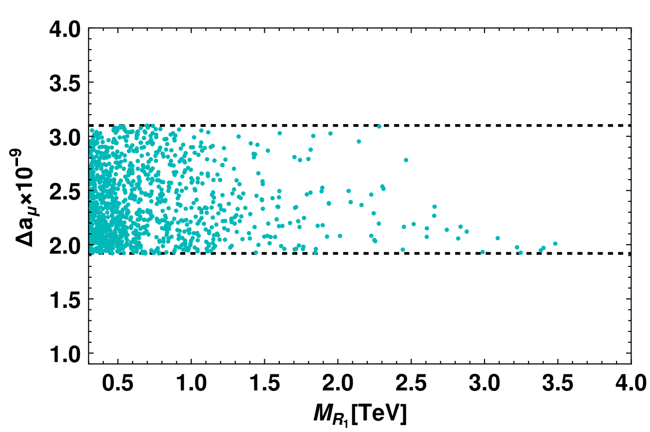

FIG. 7. The contribution of the lightest fermion triplet to muon $(g-2)$.

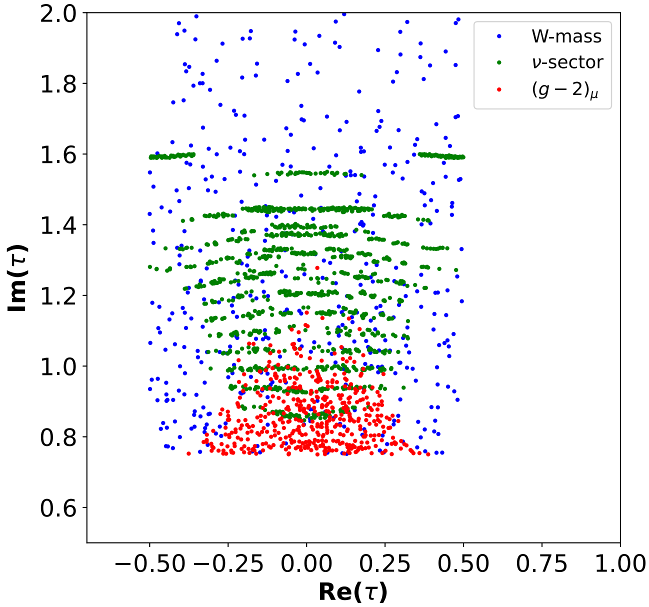

FIG. 8. The points in blue [red] color satisfy W mass $[(g-2)_\mu]$ and green color data points are for neutrino phenomenology.

neutrino phenomenology shown by green points, and muon $(g-2)$ as depicted by red points. From the figure, we obtain the ranges as $-0.27 \leq \mathrm{Re}(\tau) \leq 0.27$ and $0.84 \leq \mathrm{Im}(\tau) \leq 1.15$, which satisfy all three phenomenological aspects discussed in this paper.

VII. LEPTON FLAVOR VIOLATION

In this section, our focus is on exploring lepton flavor-violating decay as a means of establishing more precise limitations on the mass range of heavy neutrinos. Of particular interest is the highly acclaimed and rare $(\mu \to e\gamma)$ decay mode, which represents one of the most strictly restricted modes to date, with current limits set at 4.2×10^{-13} [128]. This mode is characterized by the fact that it cannot occur at the tree level and is associated with a lepton number violation. The decay widths and branching ratios for different lepton flavor-violating decays within the type-III seesaw model are presented in [129]. The heavy neutrino contribution, i.e., M_{R_1} to the one-loop branching ratio [129,130] of $\mu \to e\gamma$ is given as

$$\mathrm{Br}(\mu \to e\gamma) = \frac{3 m_e \alpha}{4\pi m_\mu}\left|(g_{D_1} y_{22})(g_{D_1} y_{22''})\frac{M_{R_1}^2}{m_h^2}\left(\frac{3}{2} + \ln\frac{M_{R_1}^2}{m_h^2}\right)\right|^2, \tag{40}$$

with α being the fine structure constant and g_{D_1} being the free parameter. y_{22} and $y_{22'}$ are the modular Yukawa couplings mentioned in Table II and m_e, m_μ, and m_h are the mass of the electron, muon, and Higgs, respectively.

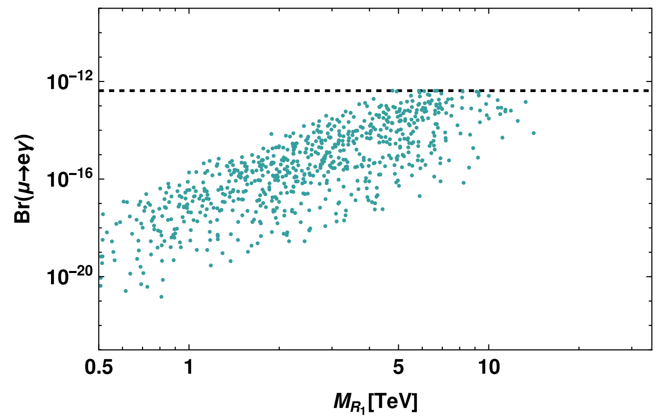

FIG. 9. Variation of $\mathrm{Br}(\mu \to e\gamma)$ against M_{R_1} (TeV), where the grid line shows the experimental upper bound.

The parameter space mentioned in Sec. IV is utilized to perform lepton flavor violation, which mutually satisfies neutrino phenomenology and other phenomena discussed in our paper. The plot for the branching ratio of $(\mu \to e\gamma)$ is depicted in Fig. 9 with respect to M_{R_1}, where the black dashed horizontal line represents the experimental upper limit [128]. From the figure, we find the upper limit on M_{R_1} as 13.4 TeV, consistent with the lepton flavor-violating (LFV) decay $\mu \to e\gamma$. This observation underscores the importance of considering the LFV bounds when investigating or constraining the limit of the lightest heavy neutrino mass, i.e., M_{R_1} in such models.

VIII. CONCLUSION

To comprehend neutrino phenomenology and explain observed oscillation data, we have considered a model including A_4' modular symmetry, employing a type-III seesaw mechanism in a minimal supersymmetric context, i.e., adding only two $SU(2)_L$ triplet fermions $(\Sigma_{R_j}^c)$. This yields a specific mass structure for Dirac and Majorana terms, which further yields a 3×3 active neutrino mass matrix. There are various modular Yukawa couplings involved in keeping the superpotential invariant under T' modular discrete symmetry for the explanation of the recent W-mass anomaly, where acquisition of the VEV by modulus τ breaks A_4' symmetry. Here, the numerical diagonalization technique lifts the workload in the analytical part, and the results are predicted following the 3σ constraint established through numerous experiments. Consequently, we obtain the sum of active neutrino masses $\sum m_{\nu_i}$ within $[0.058 - 0.12]$ eV, and mixing angles are seen to be within their respective 3σ ranges. Proceeding further, the results for δ_{CP} and Jarlskog invariant $|J_{CP}|$ are seen to be within $[142.1° - 283°]$ respectively, establishing a firm correlation. Further, from the upper bound on the $\mathrm{Br}(\mu \to e\gamma)$, the mass of the lightest right-handed neutrino is highly constrained; hence, the mass range for M_{R_1} is found to be $[0.05-13.42]$ TeV and that of M_{R_2} is in the range of $[128.8-5530]$ TeV, establishing a hierarchy between them. Advancing further, we attempt to explain the W-mass anomaly, where the presence of the scalar superpartner impacts the result, and the new mass range for W mass is 80.4335 ± 0.0094 GeV. Finally, we were successful in accommodating the results from Muon $(g-2)$ explaining the recent results.

ACKNOWLEDGMENTS

P. M. is thankful for financial support from the Prime Minister's Research Fellowship Scheme. M. K. B. would like to thank DST-Inspire for its financial support. R. M. would like to acknowledge University of Hyderabad IoE project Grant No. RC1-20-012. We gratefully acknowledge the use of the CMSD HPC facility of University of Hyderabad to carry out the computational work.

APPENDIX: T' MODULAR SYMMETRY

The modular forms of couplings required in our model are given as follows:

(i) Modular forms transforming as doublet under T' symmetry and with modular weight $k=1$,

$$Y_2^{(1)}(\tau) = \begin{pmatrix} Y_1 \\ Y_2 \end{pmatrix}, \tag{A1}$$

where Y_1 and Y_2 are the function of τ and are defined as

$$\begin{aligned} Y_1 &= \sqrt{2}e^{i7\pi/12}q^{1/3}(1+q+2q^2+2q^4+q^5+2q^6+\cdots), \\ Y_2 &= 1/3+2q+2q^3+2q^4+4q^7+2q^9+\cdots, \end{aligned} \tag{A2}$$

with $q = e^{i2\pi\tau}$.

(ii) The modular forms for the Yukawa couplings required to write the superpotential term for the neutral lepton sector are with modular weight 5,

$$Y_{2,I}^{(5)} = \begin{pmatrix} 2\sqrt{2}e^{i7\pi/12}Y_1^4Y_2 + e^{i\pi/3}Y_1Y_2^4 \\ 2\sqrt{2}e^{i7\pi/12}Y_1^3Y_2^2 + e^{i\pi/3}Y_2^5 \end{pmatrix}, \tag{A3}$$

$$Y_{2',I}^{(5)} = \begin{pmatrix} -Y_1^5 + 2(1-i)Y_1^2Y_2^3 \\ -Y_1^4Y_2 + 2(1-i)Y_1Y_2^4 \end{pmatrix}, \tag{A4}$$

$$Y_{2''}^{(5)} = \begin{pmatrix} 5e^{i\pi/6}Y_1^3Y_2^2 - (1-i)e^{i\pi/6}Y_2^5 \\ -\sqrt{2}e^{i5\pi/12}Y_1^5 - 5e^{i\pi/6}Y_1^2Y_2^3 \end{pmatrix}. \tag{A5}$$

(iii) Couplings λ_1 and λ_2 have the forms

$$\lambda_1 = Y_{3,I}^{(6)} = \begin{pmatrix} -2(1-i)Y_1^3Y_2^3 + iY_2^6 \\ -4e^{i\pi/6}Y_1^4Y_2^2 - (1-i)e^{i\pi/6}Y_1Y_2^5 \\ 2\sqrt{2}e^{i7\pi/12}Y_1^5Y_2 + e^{i\pi/3}Y_1^2Y_2^4 \end{pmatrix}, \tag{A6}$$

$$\lambda_2 = Y_{2''}^{(3)} = \begin{pmatrix} Y_1^3 + (1-i)Y_2^3 \\ -3Y_2Y_1^2 \end{pmatrix}. \tag{A7}$$

[1] R. L. Workman *et al.* (Particle Data Group), Review of particle physics, Prog. Theor. Exp. Phys. **2022**, 083C01 (2022).

[2] G. Altarelli and F. Feruglio, Discrete flavor symmetries and models of neutrino mixing, Rev. Mod. Phys. **82**, 2701 (2010).

[3] F. Feruglio, C. Hagedorn, and R. Ziegler, Lepton mixing parameters from discrete and *CP* symmetries, J. High Energy Phys. 07 (2013) 027.

[4] F. Bazzocchi, L. Merlo, and S. Morisi, Phenomenological consequences of the seesaw mechanism in S_4 based models, Phys. Rev. D **80**, 053003 (2009).

[5] S. Pramanick, Scotogenic S3 symmetric generation of realistic neutrino mixing, Phys. Rev. D **100**, 035009 (2019).

[6] D. Das and P. B. Pal, S_3 flavored left-right symmetric model of quarks, Phys. Rev. D **98**, 115001 (2018).

[7] G. J. Ding, S. F. King, and C. C. Li, Lepton mixing predictions from S_4 in the tridirect *CP* approach to two right-handed neutrino models, Phys. Rev. D **99**, 075035 (2019).

[8] D. Borah and B. Karmakar, A_4 flavour model for Dirac neutrinos: Type I and inverse seesaw, Phys. Lett. B **780**, 461 (2018).

[9] G. J. Ding, S. F. King, C. Luhn, and A. J. Stuart, Spontaneous *CP* violation from vacuum alignment in S_4 models of leptons, J. High Energy Phys. 05 (2013) 084.
[10] M. Holthausen, M. Lindner, and M. A. Schmidt, *CP* and discrete flavour symmetries, J. High Energy Phys. 04 (2013) 122.
[11] F. Feruglio, C. Hagedorn, and R. Ziegler, A realistic pattern of lepton mixing and masses from S_4 and *CP*, Eur. Phys. J. C **74**, 2753 (2014).
[12] G. J. Ding, S. F. King, and A. J. Stuart, Generalised *CP* and A_4 family symmetry, J. High Energy Phys. 12 (2013) 006.
[13] S. Weinberg, Baryon and Lepton Nonconserving Processes, Phys. Rev. Lett. **43**, 1566 (1979).
[14] R. N. Mohapatra and G. Senjanovic, Neutrino Mass and Spontaneous Parity Nonconservation, Phys. Rev. Lett. **44**, 912 (1980).
[15] S. Bilenky, *Introduction to the Physics of Massive and Mixed Neutrinos* (Springer, New York, 2018), Vol. 947.
[16] G. Branco, J. Penedo, P. M. Pereira, M. Rebelo, and J. Silva-Marcos, Type-I seesaw with eV-scale neutrinos, J. High Energy Phys. 07 (2020) 164.
[17] P. H. Gu, H. Zhang, and S. Zhou, A minimal type II seesaw model, Phys. Rev. D **74**, 076002 (2006).
[18] S. Luo and Z. z. Xing, The minimal type-II seesaw model and flavor-dependent leptogenesis, Int. J. Mod. Phys. A **23**, 3412 (2008).
[19] S. Antusch and S. F. King, Type II leptogenesis and the neutrino mass scale, Phys. Lett. B **597**, 199 (2004).
[20] W. Rodejohann, Type II seesaw mechanism, deviations from bimaximal neutrino mixing and leptogenesis, Phys. Rev. D **70**, 073010 (2004).
[21] P. H. Gu, Double type II seesaw mechanism accompanied by Dirac fermionic dark matter, Phys. Rev. D **101**, 015006 (2020).
[22] J. McDonald, N. Sahu, and U. Sarkar, Type-II seesaw at collider, lepton asymmetry and singlet scalar dark matter, J. Cosmol. Astropart. Phys. 04 (2008) 037.
[23] Y. Liao, J. Y. Liu, and G. Z. Ning, Radiative neutrino mass in type III seesaw model, Phys. Rev. D **79**, 073003 (2009).
[24] E. Ma, Pathways to Naturally Small Neutrino Masses, Phys. Rev. Lett. **81**, 1171 (1998).
[25] R. Foot, H. Lew, X. G. He, and G. C. Joshi, Seesaw neutrino masses induced by a triplet of leptons, Z. Phys. C **44**, 441 (1989).
[26] I. Dorsner and P. Fileviez Perez, Upper bound on the mass of the type III seesaw triplet in an SU(5) model, J. High Energy Phys. 06 (2007) 029.
[27] R. Franceschini, T. Hambye, and A. Strumia, Type-III seesaw at LHC, Phys. Rev. D **78**, 033002 (2008).
[28] X. G. He and S. Oh, Lepton FCNC in type III seesaw model, J. High Energy Phys. 09 (2009) 027.
[29] F. Feruglio, Are neutrino masses modular forms?, in *From My Vast Repertoire: The Legacy of Guido Altarelli*, edited by A. Levy Forte and G. Ridolfi (World Scientific, Singapore, 2018).
[30] P. Brax and M. Chemtob, Flavor changing neutral current constraints on standardlike orbifold models, Phys. Rev. D **51**, 6550 (1995).
[31] E. Dudas, S. Pokorski, and C. A. Savoy, Soft scalar masses in supergravity with horizontal $U(1)_x$ gauge symmetry, Phys. Lett. B **369**, 255 (1996).
[32] P. Binetruy and E. Dudas, Dynamical mass matrices from effective superstring theories, Nucl. Phys. **B451**, 31 (1995).
[33] X. Du and F. Wang, SUSY breaking constraints on modular flavor S_3 invariant SU(5) GUT model, J. High Energy Phys. 02 (2021) 221.
[34] S. Mishra, Neutrino mixing and leptogenesis with modular S_3 symmetry in the framework of type III seesaw, arXiv: 2008.02095.
[35] H. Okada and Y. Orikasa, Modular S_3 symmetric radiative seesaw model, Phys. Rev. D **100**, 115037 (2019).
[36] G. J. Ding, S. F. King, and X. G. Liu, Modular A_4 symmetry models of neutrinos and charged leptons, J. High Energy Phys. 09 (2019) 074.
[37] M. Abbas, Flavor masses and mixing in modular A_4 symmetry, Phys. Rev. D **103**, 056016 (2021).
[38] G. J. Ding, S. F. King, and J. N. Lu, SO(10) models with A_4 modular symmetry, J. High Energy Phys. 11 (2021) 007.
[39] M. K. Singh, S. R. Singh, and N. N. Singh, Modular A_4 symmetry in $3 + 1$ active-sterile neutrino masses and mixings, arXiv:2303.10922.
[40] S. Mishra, M. K. Behera, R. Mohanta, S. Patra, and S. Singirala, Neutrino phenomenology and dark matter in an A_4 flavour extended $B - L$ model, Eur. Phys. J. C **80**, 420 (2020).
[41] M. R. Devi, Retrieving texture zeros in $3 + 1$ active-sterile neutrino framework under the action of A_4 modular-invariants, arXiv:2303.04900.
[42] M. Kashav and S. Verma, On minimal realization of topological Lorentz structures with one-loop seesaw extensions in A_4 modular symmetry, J. Cosmol. Astropart. Phys. 03 (2023) 010.
[43] M. Kashav and S. Verma, Broken scaling neutrino mass matrix and leptogenesis based on A_4 modular invariance, J. High Energy Phys. 09 (2021) 100.
[44] G. Charalampous, S. F. King, G. K. Leontaris, and Y. L. Zhou, Flipped SU(5) with modular A_4 symmetry, Phys. Rev. D **104**, 115015 (2021).
[45] P. Chen, G. J. Ding, J. N. Lu, and J. W. F. Valle, Predictions from warped flavor dynamics based on the T' family group, Phys. Rev. D **102**, 095014 (2020).
[46] H. Okada and Y. Orikasa, Lepton mass matrix from double covering of A_4 modular flavor symmetry, Chin. Phys. C **46**, 123108 (2022).
[47] P. Beneš, H. Okada, and Y. Orikasa, Towards unification of lepton and quark mass matrices from double covering of modular A_4 flavor symmetry, arXiv:2212.07245.
[48] X. G. Liu and G. J. Ding, Neutrino masses and mixing from double covering of finite modular groups, J. High Energy Phys. 08 (2019) 134.
[49] S. J. King and S. F. King, Fermion mass hierarchies from modular symmetry, J. High Energy Phys. 09 (2020) 043.
[50] X. Wang, Lepton flavor mixing and *CP* violation in the minimal type-(I + II) seesaw model with a modular A_4 symmetry, Nucl. Phys. **B957**, 115105 (2020).
[51] J. N. Lu, X. G. Liu, and G. J. Ding, Modular symmetry origin of texture zeros and quark lepton unification, Phys. Rev. D **101**, 115020 (2020).

[52] C. C. Li, X. G. Liu, and G. J. Ding, Modular symmetry at level 6 and a new route towards finite modular groups, J. High Energy Phys. 10 (2021) 238.
[53] J. Gogoi, N. Gautam, and M. K. Das, Neutrino masses and mixing in minimal inverse seesaw using A_4 modular symmetry, Int. J. Mod. Phys. A **38**, 2350022 (2023).
[54] T. Kobayashi, T. Nomura, and T. Shimomura, Type II seesaw models with modular A_4 symmetry, Phys. Rev. D **102**, 035019 (2020).
[55] T. Nomura, H. Okada, and S. Patra, An inverse seesaw model with A_4-modular symmetry, Nucl. Phys. **B967**, 115395 (2021).
[56] T. Asaka, Y. Heo, T. H. Tatsuishi, and T. Yoshida, Modular A_4 invariance and leptogenesis, J. High Energy Phys. 01 (2020) 144.
[57] M. K. Behera, S. Mishra, S. Singirala, and R. Mohanta, Implications of A_4 modular symmetry on neutrino mass, mixing and leptogenesis with linear seesaw, Phys. Dark Universe **36**, 101027 (2022).
[58] M. K. Behera, S. Singirala, S. Mishra, and R. Mohanta, A modular A_4 symmetric scotogenic model for neutrino mass and dark matter, J. Phys. G **49**, 035002 (2022).
[59] P. Mishra, M. K. Behera, P. Panda, and R. Mohanta, Type III seesaw under A_4 modular symmetry with leptogenesis, Eur. Phys. J. C **82**, 1115 (2022).
[60] J. Penedo and S. Petcov, Lepton masses and mixing from modular S_4 symmetry, Nucl. Phys. **B939**, 292 (2019).
[61] P. Novichkov, J. Penedo, S. Petcov, and A. Titov, Modular S_4 models of lepton masses and mixing, J. High Energy Phys. 04 (2019) 005.
[62] H. Okada and Y. Orikasa, Neutrino mass model with a modular S_4 symmetry, arXiv:1908.08409.
[63] I. de Medeiros Varzielas and J. a. Lourenço, Two A5 modular symmetries for golden ratio 2 mixing, Nucl. Phys. **B984**, 115974 (2022).
[64] F. J. de Anda and S. F. King, Modular flavour symmetry and orbifolds, arXiv:2304.05958.
[65] S. F. King and Y. L. Zhou, Twin modular S_4 with SU(5) GUT, J. High Energy Phys. 04 (2021) 291.
[66] P. P. Novichkov, J. T. Penedo, S. T. Petcov, and A. V. Titov, Modular A_5 symmetry for flavour model building, J. High Energy Phys. 04 (2019) 174.
[67] X. Wang, B. Yu, and S. Zhou, Double covering of the modular A_5 group and lepton flavor mixing in the minimal seesaw model, Phys. Rev. D **103**, 076005 (2021).
[68] M. K. Behera and R. Mohanta, Inverse seesaw in A_5' modular symmetry, J. Phys. G **49**, 045001 (2022).
[69] M. K. Behera and R. Mohanta, Linear seesaw in A_5' modular symmetry with leptogenesis, Front. Phys. **10**, 854595 (2022).
[70] X. Wang and S. Zhou, Explicit perturbations to the stabilizer $\tau = i$ of modular A_5' symmetry and leptonic CP violation, J. High Energy Phys. 07 (2021) 093.
[71] X. G. Liu and G. J. Ding, Neutrino masses and mixing from double covering of finite modular groups, J. High Energy Phys. 08 (2019) 134.
[72] T. Aaltonen *et al.* (CDF Collaboration), High-precision measurement of the W boson mass with the CDF II detector, Science **376**, 170 (2022).
[73] P. A. Zyla *et al.* (Particle Data Group), Review of particle physics, Prog. Theor. Exp. Phys. **2020**, 083C01 (2020).
[74] T. A. Chowdhury, J. Heeck, A. Thapa, and S. Saad, W boson mass shift and muon magnetic moment in the Zee model, Phys. Rev. D **106**, 035004 (2022).
[75] R. Dcruz and A. Thapa, W boson mass shift, dark matter, and $(g-2)_\ell$ in a scotogenic-Zee model, Phys. Rev. D **107**, 015002 (2023).
[76] D. Borah, S. Mahapatra, D. Nanda, and N. Sahu, Type II Dirac seesaw with observable ΔN_{eff} in the light of W-mass anomaly, Phys. Lett. B **833**, 137297 (2022).
[77] D. Borah, S. Mahapatra, and N. Sahu, Singlet-doublet fermion origin of dark matter, neutrino mass and W-mass anomaly, Phys. Lett. B **831**, 137196 (2022).
[78] S. Heinemeyer, CDF measurement of M_W: Theory implications, arXiv:2207.14809.
[79] S. Baek, Implications of CDF W-mass and $(g-2)_\mu$ on $U(1)_{L_\mu - L_\tau}$ model, arXiv:2204.09585.
[80] K. I. Nagao, T. Nomura, and H. Okada, A model explaining the new CDF II W boson mass linking to muon $g-2$ and dark matter, Eur. Phys. J. Plus **138**, 365 (2023).
[81] A. Batra, K. A. ShivaSankar, S. Mandal, and R. Srivastava, W boson mass in singlet-triplet scotogenic dark matter model, arXiv:2204.09376.
[82] J. Cao, L. Meng, L. Shang, S. Wang, and B. Yang, Interpreting the W-mass anomaly in vectorlike quark models, Phys. Rev. D **106**, 055042 (2022).
[83] P. Athron, A. Fowlie, C. T. Lu, L. Wu, Y. Wu, and B. Zhu, Hadronic uncertainties versus new physics for the W boson mass and muon $g-2$ anomalies, Nat. Commun. **14**, 659 (2023).
[84] K. Sakurai, F. Takahashi, and W. Yin, Singlet extensions and W boson mass in light of the CDF II result, Phys. Lett. B **833**, 137324 (2022).
[85] E. Ma, Type III neutrino seesaw, freeze-in long-lived dark matter, and the W mass shift, Phys. Lett. B **833**, 137327 (2022).
[86] J. Heeck, W-boson mass in the triplet seesaw model, Phys. Rev. D **106**, 015004 (2022).
[87] O. Popov and R. Srivastava, The triplet Dirac seesaw in the view of the recent CDF-II W-mass anomaly, Phys. Lett. B **840**, 137837 (2023).
[88] S. Kanemura and K. Yagyu, Implication of the W boson mass anomaly at CDF II in the Higgs triplet model with a mass difference, Phys. Lett. B **831**, 137217 (2022).
[89] D. Schultz, Notes on modular forms, https://faculty.math.illinois.edu//schult25/ModFormNotes.pdf (2015).
[90] P. P. Novichkov, J. T. Penedo, and S. T. Petcov, Double cover of modular S_4 for flavour model building, Nucl. Phys. **B963**, 115301 (2021).
[91] X. G. Liu, C. Y. Yao, and G. J. Ding, Modular invariant quark and lepton models in double covering of S_4 modular group, Phys. Rev. D **103**, 056013 (2021).
[92] S. Kikuchi, T. Kobayashi, H. Otsuka, S. Takada, and H. Uchida, Modular symmetry by orbifolding magnetized $T^2 \times T^2$: Realization of double cover of Γ_N, J. High Energy Phys. 11 (2020) 101.
[93] S. Antusch and V. Maurer, Running quark and lepton parameters at various scales, J. High Energy Phys. 11 (2013) 115.
[94] H. Okada and M. Tanimoto, Towards unification of quark and lepton flavors in A_4 modular invariance, Eur. Phys. J. C **81**, 52 (2021).

[95] F. Björkeroth, F. J. de Anda, I. de Medeiros Varzielas, and S. F. King, Towards a complete $A_4 \times SU(5)$ SUSY GUT, J. High Energy Phys. 06 (2015) 141.
[96] I. Esteban, M. C. Gonzalez-Garcia, M. Maltoni, T. Schwetz, and A. Zhou, The fate of hints: Updated global analysis of three-flavor neutrino oscillations, J. High Energy Phys. 09 (2020) 178.
[97] NuFIT-5.2, Nufit, www.nu-fit.org (2022).
[98] N. Aghanim *et al.* (Planck Collaboration), Planck 2018 results. VI. Cosmological parameters, Astron. Astrophys. **641**, A6 (2020).
[99] S. Vagnozzi, E. Giusarma, O. Mena, K. Freese, M. Gerbino, S. Ho, and M. Lattanzi, Unveiling ν secrets with cosmological data: Neutrino masses and mass hierarchy, Phys. Rev. D **96**, 123503 (2017).
[100] S. Roy Choudhury and S. Hannestad, Updated results on neutrino mass and mass hierarchy from cosmology with Planck 2018 likelihoods, J. Cosmol. Astropart. Phys. 07 (2020) 037.
[101] A. Ghoshal, N. Okada, S. Okada, D. Raut, Q. Shafi, and A. Thapa, Type III seesaw with R-parity violation in light of m_W (CDF), Nucl. Phys. **B989**, 116099 (2023).
[102] S. P. Martin, A supersymmetry primer, Adv. Ser. Dir. High Energy Phys. **18**, 1 (1998).
[103] S. Di Chiara and K. Hsieh, Triplet extended supersymmetric standard model, Phys. Rev. D **78**, 055016 (2008).
[104] T. Aoyama, M. Hayakawa, T. Kinoshita, and M. Nio, Complete Tenth-Order QED Contribution to the Muon $g-2$, Phys. Rev. Lett. **109**, 111808 (2012).
[105] T. Aoyama, T. Kinoshita, and M. Nio, Theory of the anomalous magnetic moment of the electron, Atoms **7**, 28 (2019).
[106] A. Czarnecki, W. J. Marciano, and A. Vainshtein, Refinements in electroweak contributions to the muon anomalous magnetic moment, Phys. Rev. D **67**, 073006 (2003).
[107] C. Gnendiger, D. Stöckinger, and H. Stöckinger-Kim, The electroweak contributions to $(g-2)_\mu$ after the Higgs boson mass measurement, Phys. Rev. D **88**, 053005 (2013).
[108] M. Davier, A. Hoecker, B. Malaescu, and Z. Zhang, Reevaluation of the hadronic vacuum polarisation contributions to the standard model predictions of the muon $g-2$ and $\alpha(m_Z^2)$ using newest hadronic cross-section data, Eur. Phys. J. C **77**, 827 (2017).
[109] A. Keshavarzi, D. Nomura, and T. Teubner, Muon $g-2$ and $\alpha(M_Z^2)$: A new data-based analysis, Phys. Rev. D **97**, 114025 (2018).
[110] G. Colangelo, M. Hoferichter, and P. Stoffer, Two-pion contribution to hadronic vacuum polarization, J. High Energy Phys. 02 (2019) 006.
[111] M. Hoferichter, B. L. Hoid, and B. Kubis, Three-pion contribution to hadronic vacuum polarization, J. High Energy Phys. 08 (2019) 137.
[112] M. Davier, A. Hoecker, B. Malaescu, and Z. Zhang, A new evaluation of the hadronic vacuum polarisation contributions to the muon anomalous magnetic moment and to $\boldsymbol{\alpha}(m_Z^2)$, Eur. Phys. J. C **80**, 241 (2020).
[113] A. Keshavarzi, D. Nomura, and T. Teubner, The $g-2$ of charged leptons, $\alpha(M_Z^2)$ and the hyperfine splitting of muonium, Phys. Rev. D **101**, 014029 (2020).
[114] A. Kurz, T. Liu, P. Marquard, and M. Steinhauser, Hadronic contribution to the muon anomalous magnetic moment to next-to-next-to-leading order, Phys. Lett. B **734**, 144 (2014).
[115] K. Melnikov and A. Vainshtein, Hadronic light-by-light scattering contribution to the muon anomalous magnetic moment revisited, Phys. Rev. D **70**, 113006 (2004).
[116] P. Masjuan and P. Sánchez-Puertas, Pseudoscalar-pole contribution to the $(g_\mu - 2)$: A rational approach, Phys. Rev. D **95**, 054026 (2017).
[117] G. Colangelo, M. Hoferichter, M. Procura, and P. Stoffer, Dispersion relation for hadronic light-by-light scattering: Two-pion contributions, J. High Energy Phys. 04 (2017) 161.
[118] M. Hoferichter, B. L. Hoid, B. Kubis, S. Leupold, and S. P. Schneider, Dispersion relation for hadronic light-by-light scattering: Pion pole, J. High Energy Phys. 10 (2018) 141.
[119] A. Gérardin, H. B. Meyer, and A. Nyffeler, Lattice calculation of the pion transition form factor with $N_f = 2+1$ Wilson quarks, Phys. Rev. D **100**, 034520 (2019).
[120] J. Bijnens, N. Hermansson-Truedsson, and A. Rodríguez-Sánchez, Short-distance constraints for the HLbL contribution to the muon anomalous magnetic moment, Phys. Lett. B **798**, 134994 (2019).
[121] G. Colangelo, F. Hagelstein, M. Hoferichter, L. Laub, and P. Stoffer, Longitudinal short-distance constraints for the hadronic light-by-light contribution to $(g-2)_\mu$ with large-N_c Regge models, J. High Energy Phys. 03 (2020) 101.
[122] T. Blum, N. Christ, M. Hayakawa, T. Izubuchi, L. Jin, C. Jung, and C. Lehner, The Hadronic Light-by-Light Scattering Contribution to the Muon Anomalous Magnetic Moment from Lattice QCD, Phys. Rev. Lett. **124**, 132002 (2020).
[123] G. Colangelo, M. Hoferichter, A. Nyffeler, M. Passera, and P. Stoffer, Remarks on higher-order hadronic corrections to the muon $g-2$, Phys. Lett. B **735**, 90 (2014).
[124] T. Albahri *et al.* (Muon $g-2$ Collaboration), Measurement of the anomalous precession frequency of the muon in the Fermilab Muon $g-2$ experiment, Phys. Rev. D **103**, 072002 (2021).
[125] G. W. Bennett *et al.* (Muon $g-2$ Collaboration), Final report of the muon E821 anomalous magnetic moment measurement at BNL, Phys. Rev. D **73**, 072003 (2006).
[126] B. Abi *et al.* (Muon $g-2$ Collaboration), Measurement of the Positive Muon Anomalous Magnetic Moment to 0.46 ppm, Phys. Rev. Lett. **126**, 141801 (2021).
[127] K. Kannike, M. Raidal, D. M. Straub, and A. Strumia, Anthropic solution to the magnetic muon anomaly: The charged see-saw, J. High Energy Phys. 02 (2012) 106.
[128] A. M. Baldini *et al.* (MEG Collaboration), Search for the lepton flavour violating decay $\mu^+ \to e^+\gamma$ with the full dataset of the MEG experiment, Eur. Phys. J. C **76**, 434 (2016).
[129] A. Abada, C. Biggio, F. Bonnet, M. B. Gavela, and T. Hambye, $\mu \to e\gamma$ and $\tau \to l\gamma$ decays in the fermion triplet seesaw model, Phys. Rev. D **78**, 033007 (2008).
[130] D. Chang, W. S. Hou, and W. Y. Keung, Two loop contributions of flavor changing neutral Higgs bosons to $\mu \to e\gamma$, Phys. Rev. D **48**, 217 (1993).